Impact of gain saturation on the mode instability threshold in high-power fiber amplifiers

Hansen, Kristian Rymann; Lægsgaard, Jesper

Published in:
Optics Express

Link to article, DOI:
10.1364/OE.22.011267

Publication date:
2014

Document Version
Publisher's PDF, also known as Version of record

Impact of gain saturation on the mode instability threshold in high-power fiber amplifiers

Kristian Rymann Hansen* **and Jesper Lægsgaard**

Department of Photonics Engineering, Technical University of Denmark Bldg. 343, DK-2800 Kgs. Lyngby, Denmark

*kryh@fotonik.dtu.dk

Abstract: We present a coupled-mode model of transverse mode instability in high-power fiber amplifiers, which takes the effect of gain saturation into account. The model provides simple semi-analytical formulas for the mode instability threshold, which are valid also for highly saturated amplifiers. The model is compared to recently published detailed numerical simulations of mode instability, and we find reasonably good agreement with our simplified coupled-mode model.

OCIS codes: (060.2320) Fiber optics amplifiers and oscillators; (060.4370) Nonlinear optics, fibers; (140.6810) Thermal effects; (190.3100) Instabilities and chaos; (190.4370) Nonlinear optics, fibers.

References and links

1. T. Eidam, C. Wirth, C. jauregui, F. Stutzki, F. Jansen, H.-J. Otto, O. Schmidt, T. Schreiber, J. Limpert, and A. Tünnermann, "Experimental observations of the threshold-like onset of mode instabilities in high power fiber amplifiers," Opt. Express **19**, 13218–13224 (2011).
2. F. Stutzki, H.-J. Otto, F. Jansen, C. Gaida, C. Jauregui, J. Limpert, and A. Tünnermann, "High-speed modal decomposition of mode instabilities in high-power fiber lasers," Opt. Lett. **36**, 4572–4574 (2011).
3. H.-J. Otto, F. Stutzki, F. Jansen, T. Eidam, C. Jauregui, J. Limpert, and A. Tünnermann, "Temporal dynamics of mode instabilities in high-power fiber lasers and amplifiers," Opt. Express **20**, 15710–15722 (2012).
4. M. M. Johansen, M. Laurila, M. D. Maack, D. Noordegraaf, C. Jakobsen, T. T. Alkeskjold, and J. Lægsgaard, "Frequency resolved transverse mode instability in rod fiber amplifiers," Opt. Express **21**, 21847–21856 (2013).
5. C. Jauregui, T. Eidam, J. Limpert, and A. Tünnermann, "Impact of modal interference on the beam quality of high-power fiber amplifiers," Opt. Express **19**, 3258–3271 (2011).
6. A. V. Smith, and J. J. Smith, "Mode instability in high power fiber amplifiers," Opt. Express **19**, 10180–10192 (2011).
7. A. V. Smith, and J. J. Smith, "Influence of pump and seed modulation on the mode instability thresholds of fiber amplifiers," Opt. Express **20**, 24545–24558 (2012).
8. B. Ward, C. Robin, and I. Dajani, "Origin of thermal modal instabilities in large mode area fiber amplifiers," Opt. Express **20**, 11407–11422 (2012).
9. B. Ward, "Modeling of transient modal instability in fiber amplifiers," Opt. Express **21**, 12053–12067 (2013).
10. S. Naderi, I. Dajani, T. Madden, and C. Robin, "Investigations of modal instabilities in fiber amplifiers through detailed numerical simulations," Opt. Express **21**, 16111–16129 (2013).
11. K. R. Hansen, T. T. Alkeskjold, J. Broeng, and J. Lægsgaard, "Thermally induced mode coupling in rare-earth doped fiber amplifiers," Opt. Lett. **37**, 2382–2384 (2012).
12. K. R. Hansen, T. T. Alkeskjold, J. Broeng, and J. Lægsgaard, "Theoretical analysis of mode instability in high-power fiber amplifiers," Opt. Express **21**, 1944–1971 (2013).
13. A. V. Smith, and J. J. Smith, "Increasing mode instability thresholds of fiber amplifiers by gain saturation," Opt. Express **21**, 15168–15182 (2013).

#205315 - $15.00 USD Received 24 Jan 2014; revised 4 Apr 2014; accepted 25 Apr 2014; published 2 May 2014

1. Introduction

The recent discovery of transverse mode instability (TMI) in high-power fiber amplifiers [1] has motivated experimental [2–4] and theoretical [5–13] efforts to characterize and explain this phenomenon. TMI manifests itself as an instability in which the signal power fluctuates on a ms timescale between the fundamental mode (FM) and the first few higher-order modes (HOMs) when the average signal power is increased above a certain threshold. The experimental and theoretical research into this phenomenon has provided strong evidence that the underlying physical mechanism responsible for TMI is a form of stimulated thermal Rayleigh scattering (STRS) [7], caused by quantum defect heating of the active fiber. Essentially, the presence of light in the FM and HOM of a multimode active fiber results in a mode beating pattern in the signal intensity, which leads to a corresponding spatially and temporally oscillating thermal profile. Since the refractive index of silica is temperature dependent, a thermally induced long period grating (LPG) is generated, which has the correct period to couple the two modes. Due to the fact that this thermal nonlinearity is extremely slow, with a typical timescale of several ms, a phase-lag between this LPG and the mode beating pattern will exist if the latter changes due to noise or transients in the signal, which is necessary to induce strong coupling between the modes [6].

Several numerical models of TMI have been based on variants of the beam propagation method (BPM) [5–10]. While such numerical simulations can potentially include all relevant physical effects, the need to include the temporal dynamics, either by performing the simulation in the time domain or by including several frequency components in the frequency domain, leads to a numerically very intensive problem. Indeed, these numerical codes have so far employed various approximations, such as limiting the number of frequency components in the simulation [6, 7], expanding the electric field in a small number of transverse modes [8, 10] or limiting the simulation time in time domain algorithms [9].

In previous publications, we have proposed an alternative model of TMI in terms of a coupled-mode model [11, 12]. While this model has the advantage of numerical efficiency, and even allows for semi-analytical solutions, it does rely on a number of approximations, the most limiting of which is the neglect of spatiotemporal oscillations in the gain coefficient due to gain saturation. This approximation leads to an overestimate of the strength of the thermally induced LPG, which in turn leads to an underestimate of the TMI threshold power. In this paper, we show how this important effect can be included to lowest order in a coupled-mode formulation of TMI in fiber amplifiers.

2. Coupled-mode model

We consider the signal field in the scalar approximation written as a superposition of the FM and first HOM of the fiber, since typically only the first HOM is involved in TMI [3, 12]

$$E(\mathbf{r},t) = a_1(z)\psi_1(\mathbf{r}_\perp)e^{-i(\beta_1 z-\omega_1 t)} + a_2(z)\psi_2(\mathbf{r}_\perp)e^{-i(\beta_2 z-\omega_2 t)}. \tag{1}$$

Here, $a_{1,2}$ are the amplitudes of the FM and HOM, respectively, with normalized mode profiles $\psi_{1,2}$ and propagation constants $\beta_{1,2}$. Note that the frequency of the light in the HOM ω_2 differs from the light in the FM ω_1. We consider here that the frequency shifted light in the HOM is due to either intensity or quantum noise, and we shall later integrate over ω_2 to obtain the total power in the HOM. The electric field obeys the scalar wave equation

$$\frac{\partial^2 E}{\partial z^2} + \nabla_\perp^2 E - \frac{\varepsilon(\mathbf{r},t)}{c^2}\frac{\partial^2 E}{\partial t^2} = 0, \tag{2}$$

#205315 - $15.00 USD Received 24 Jan 2014; revised 4 Apr 2014; accepted 25 Apr 2014; published 2 May 2014

where the relative permittivity is given by

$$\varepsilon(\mathbf{r},t) = \varepsilon_f(\mathbf{r}_\perp) + i\frac{g(\mathbf{r})\sqrt{\varepsilon_f}}{k} + \Delta\varepsilon(\mathbf{r},t). \tag{3}$$

The relative permittivity of the unperturbed fiber is given by ε_f, the perturbation due to the thermal nonlinearity is given by $\Delta\varepsilon = \eta\Delta T$ and the gain coefficient is denoted by g.

The change in temperature relative to the cooling fluid ΔT obeys the heat equation

$$\rho C\frac{\partial \Delta T}{\partial t} - \kappa\nabla_\perp^2 \Delta T(\mathbf{r},t) = Q(\mathbf{r},t), \tag{4}$$

subject to the convection cooling boundary condition

$$\kappa\frac{\partial \Delta T}{\partial r} + h_q \Delta T(\mathbf{r},t) = 0, \tag{5}$$

where ρ is the density, C is the specific heat capacity, and κ is the thermal conductivity of the fiber material. These are assumed to be constant throughout the fiber cross section and independent of temperature. The convection coefficient of the coolant is denoted by h_q. Note that we have assumed that the longitudinal heat diffusion is negligible compared to the transverse heat diffusion in the heat equation. This approximation was tested numerically in [8], where it was found that TMI is not strongly dependent on the longitudinal heat diffusion. In fibers with a mode beat length comparable to the core radius, this approximation may break down and longitudinal heat diffusion would need to be taken into account. Assuming a steady-state solution to the rate equations of the gain medium, the heat load is given by

$$Q(\mathbf{r},t) = \left(\frac{\lambda_s}{\lambda_p} - 1\right) g(I) I(\mathbf{r},t), \tag{6}$$

where λ_s is the signal wavelength, λ_p is the pump wavelength, I is the signal intensity and the gain coefficient g is given by

$$g(I) = \frac{g_0}{1 + I/I_{sat}}, \tag{7}$$

where g_0 is the small signal gain and I_{sat} is the saturation intensity, both of which are dependent on the pump power. The intensity of the signal can be written

$$I(\mathbf{r},t) = I_0(\mathbf{r}) + \tilde{I}(\mathbf{r},t), \tag{8}$$

where I_0 is a slowly varying component given by

$$I_0(\mathbf{r}) = |p_1(z)|^2 |\psi_1(\mathbf{r}_\perp)|^2 + |p_2(z)|^2 |\psi_2(\mathbf{r}_\perp)|^2, \tag{9}$$

and $\tilde{I}$ is a spatially and temporally oscillating component given by

$$\tilde{I}(\mathbf{r},t) = p_1(z)p_2(z)^* \psi_1(\mathbf{r}_\perp)\psi_2(\mathbf{r}_\perp)^* e^{-i(\Delta\beta z - \Delta\omega t)} + \text{c.c.} \tag{10}$$

We have introduced the difference in propagation constant $\Delta\beta = \beta_1 - \beta_2$ and frequency $\Delta\omega = \omega_1 - \omega_2$, as well as the scaled mode amplitudes

$$p_i(z) = \sqrt{\frac{1}{2} n_c \varepsilon_0 c a_i(z)}, \tag{11}$$

where n_c is the core refractive index of the fiber. It is clear from Eq. (6) that the presence of light in the HOM leads to an oscillating heat load Q, which results in a thermally induced LPG.

#205315 - $15.00 USD Received 24 Jan 2014; revised 4 Apr 2014; accepted 25 Apr 2014; published 2 May 2014

However, it is also clear from Eq. (7) that the strength of this grating is reduced if the gain is highly saturated, since the maxima in the mode beating intensity pattern coincide with minima in the gain coefficient under the assumption of fixed g_0 and I_{sat}. In the extreme case where $I >> I_{sat}$, we see that the oscillations in the heat load disappear, and no LPG is induced.

Assuming that the fiber amplifier is operating below the TMI threshold, where the excitation of the HOM is small compared to the FM, we can expand Eq. (6) in powers of $\tilde{I}/(I_0 + I_{sat})$ which yields

$$Q(\mathbf{r},t) \approx \left(\frac{\lambda_s}{\lambda_p} - 1\right) \frac{g_0}{1 + I_0/I_{sat}} \left[I_0 + I_{sat} \left(\frac{\tilde{I}}{I_0 + I_{sat}} - \left(\frac{\tilde{I}}{I_0 + I_{sat}} \right)^2 \right) \right]. \tag{12}$$

Provided that the HOM excitation is weak compared to the FM excitation, which is the case when the amplifier is not operating above the TMI threshold power, we can neglect higher order terms in the expansion and keep only the first order term. The approximate heat load is thus given to first order as

$$Q(\mathbf{r},t) \approx \left(\frac{\lambda_s}{\lambda_p} - 1\right) \frac{g_0}{1 + I_0/I_{sat}} \left(I_0 + \frac{\tilde{I}}{1 + I_0/I_{sat}} \right). \tag{13}$$

A similar expansion of the heat load was considered in [10] to show that TMI does not occur under steady-state conditions, as also pointed out in [6].

As in [11] we can now derive coupled-mode equations, which are valid also for non-steady-state conditions, for the mode amplitudes p_i by solving Eq. (4) in the frequency domain using an appropriate Green's function

$$\Delta T(\mathbf{r},\omega) = \frac{1}{\kappa} \iint G(\mathbf{r}_\perp, \mathbf{r}'_\perp, \omega) Q(\mathbf{r}', \omega) \mathrm{d}^2 \mathbf{r}'_\perp. \tag{14}$$

In this paper, we shall consider only step-index fiber (SIF) models, and we assume that the thermal conductivity κ and thermo-optic coefficient η are constant throughout the fiber cross section. In this case, the appropriate Green's function is the same as given in [12]. The resulting coupled-mode equations in terms of mode power $P_i = |p_i|^2$ are

$$\frac{\partial P_1}{\partial z} = -g_0(z)\chi(z,\Delta\omega)P_2P_1 + \Gamma_1 \tilde{g}(z) P_1, \tag{15a}$$

$$\frac{\partial P_2}{\partial z} = g_0(z)\chi(z,\Delta\omega)P_2P_1 + \Gamma_2 \tilde{g}(z) P_2. \tag{15b}$$

We have introduced an approximate gain coefficient $\tilde{g}$ in the last term on the rhs. of Eqns. (15), in which spatial hole burning is only approximately taken into account. It is given by

$$\tilde{g} = \frac{g_0}{1 + \Gamma_1 P_1/P_{sat}}, \tag{16}$$

where $P_{sat} = I_{sat} A_d$ is the saturation power, A_d is the area of the doped region, and Γ_i are overlap integrals with the doped region given by

$$\Gamma_i = \iint_{A_d} |\psi_i(\mathbf{r}_\perp)|^2 \mathrm{d}^2 \mathbf{r}_\perp. \tag{17}$$

This approximation is valid provided that the FM profile does not vary much over the doped region of the fiber core, and is a good approximation for weakly-guiding, nearly single-mode fibers.

#205315 - $15.00 USD Received 24 Jan 2014; revised 4 Apr 2014; accepted 25 Apr 2014; published 2 May 2014

The nonlinear gain coefficient χ is given by

$$\chi(z,\Delta\omega) = \frac{\eta k^2}{\kappa\beta_1}\left(1-\frac{\lambda_s}{\lambda_p}\right)\mathrm{Im}\left[A(z,\Delta\omega)\right], \tag{18}$$

where k is the vacuum wavenumber of the signal. The quantity A is given by the integral

$$A(z,\Delta\omega) = \int \psi_1(\mathbf{r}_\perp)^*\psi_2(\mathbf{r}_\perp)\int_{A_d} G(\mathbf{r}_\perp,\mathbf{r}'_\perp,\Delta\omega)\frac{\psi_1(\mathbf{r}'_\perp)\psi_2(\mathbf{r}'_\perp)^*}{\left(1+P_1(z)|\psi_1(\mathbf{r}'_\perp)|^2/I_{sat}\right)^2}\mathrm{d}^2\mathbf{r}'_\perp\mathrm{d}^2\mathbf{r}_\perp, \tag{19}$$

which can be calculated using standard numerical quadrature methods for any fiber for which the thermal Green's function and mode functions are known. It is clear from Eq. (19) that the nonlinear gain coefficient χ is reduced as the signal power becomes comparable to the saturation power. This is due to the above mentioned reduction in the strength of the thermally induced LPG. While it is possible to calculate the integral in Eq. (19) for each z in a numerical solution of the coupled-mode equations, we shall show that a more efficient approach is to approximate the inner integral in Eq. (19) so that the integral only need to be calculated once. We assume that the mode function of the FM ψ_1 in the denominator of the integrand can be approximated to be constant over the doped region, such that

$$|\psi_1(\mathbf{r}_\perp)|^2 \approx \frac{1}{A_d}\iint_{A_d}|\psi_1(\mathbf{r}_\perp)|^2\mathrm{d}^2\mathbf{r}_\perp \tag{20}$$

in the denominator of Eq. (19). We hereby obtain the approximate expression

$$A(z,\Delta\omega) \approx \left(\frac{\tilde{g}(z)}{g_0(z)}\right)^2\int \psi_1(\mathbf{r}_\perp)^*\psi_2(\mathbf{r}_\perp)\int_{A_d} G(\mathbf{r}_\perp,\mathbf{r}'_\perp,\Delta\omega)\psi_1(\mathbf{r}'_\perp)\psi_2(\mathbf{r}'_\perp)^*\mathrm{d}^2\mathbf{r}'_\perp\mathrm{d}^2\mathbf{r}_\perp. \tag{21}$$

With this approximation, the coupled-mode equations become

$$\frac{\partial P_1}{\partial z} = -\tilde{g}(z)\tilde{\chi}(z,\Delta\omega)P_2P_1+\Gamma_1\tilde{g}(z)P_1, \tag{22a}$$

$$\frac{\partial P_2}{\partial z} = \tilde{g}(z)\tilde{\chi}(z,\Delta\omega)P_2P_1+\Gamma_2\tilde{g}(z)P_2, \tag{22b}$$

where the approximate nonlinear gain coefficient $\tilde{\chi}$ is given by

$$\tilde{\chi}(z,\Delta\omega) = \frac{\tilde{g}(z)}{g_0(z)}\chi_0(\Delta\omega) \tag{23}$$

and χ_0 is the same nonlinear gain coefficient derived in [11, 12]

$$\chi_0 = \frac{\eta k^2}{\kappa\beta_1}\left(1-\frac{\lambda_s}{\lambda_p}\right)\mathrm{Im}\left[A_0(z,\Delta\omega)\right], \tag{24}$$

with

$$A_0(\Delta\omega) = \int \psi_1(\mathbf{r}_\perp)^*\psi_2(\mathbf{r}_\perp)\int_{A_d} G(\mathbf{r}_\perp,\mathbf{r}'_\perp,\Delta\omega)\psi_1(\mathbf{r}'_\perp)\psi_2(\mathbf{r}'_\perp)^*\mathrm{d}^2\mathbf{r}'_\perp\mathrm{d}^2\mathbf{r}_\perp. \tag{25}$$

We note that the approximate coupled-mode equations given by Eqns. (22) are similar to the ones derived in [11], except for the fact that the nonlinear gain coefficient is now z-dependent and has a reduced value due to the effect of gain saturation.

In order to check the approximation used in obtaining the approximate expression for A given in Eq. (21), we compare the value of χ calculated using the exact expression in Eq. (19) and the

#205315 - $15.00 USD Received 24 Jan 2014; revised 4 Apr 2014; accepted 25 Apr 2014; published 2 May 2014

Table 1. Fiber parameters for Fiber A and B.

Core radius	R_{core}	20 μm
Cladding radius	R_{clad}	100 μm
Doped radius	R_{doped}	20 μm / 15 μm
Outer radius	R_{outer}	500 μm
Core index	n_{core}	1.45
V parameter	V	3
Dopant concentration	ρ_{Yb}	3×10^{7} μm^{-3}
Fiber length	L	1.5 m / 3 m
Signal wavelength	λ_s	1032 nm
Pump wavelength	λ_p	975 nm
Convection coefficient	h_q	1000 W/(m^{2}K)
Thermo-optic coefficient	η	3.5×10^{-5} K^{-1}
Thermal conductivity	κ	1.4 W/(Km)
Volumetric heat capacity	ρC	1.67×10^{6} J/(Km^3)

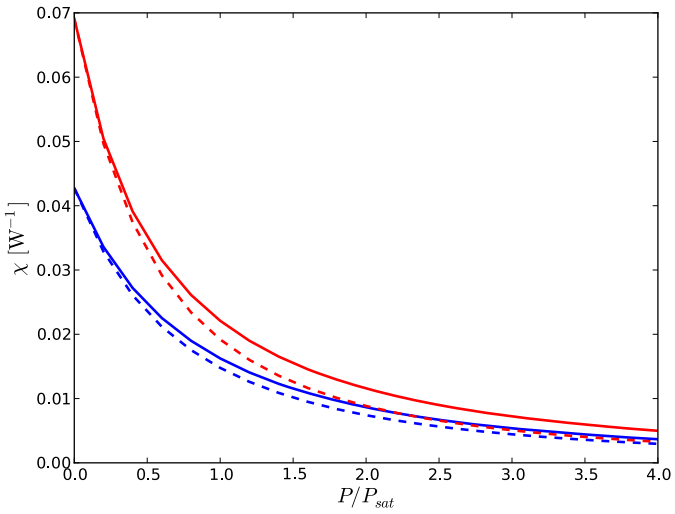

Fig. 1. Nonlinear gain coefficient χ as a function of P/P_{sat} for a fixed frequency difference $\Delta\nu = 1$ kHz. The solid curves are calculated using the exact expression for A, while the dashed curves are calculated using the approximate expression for A. The red curves are the results for Fiber A with a doped radius of 20 μm, while the blue curves are for Fiber B with a doped radius of 15 μm. As expected, the nonlinear gain coefficient decreases with increasing signal power due to the effect of gain saturation. The approximate calculation of χ remains reasonable as the signal power is increased, especially for Fiber B with the reduced doped area.

approximate expression given in Eq. (21) for a typical double-clad SIF and a range of values of P_1/P_{sat}. Two SIFs, called Fiber A and Fiber B, with different radii of the doped region are considered to investigate the effect of a reduced doped region. The relevant fiber parameters are given in Table 1 and the result is shown in Fig. 1. It is clear that the nonlinear gain coefficient decreases significantly as the signal power becomes comparable to the saturation power, which

#205315 - $15.00 USD Received 24 Jan 2014; revised 4 Apr 2014; accepted 25 Apr 2014; published 2 May 2014

is due to the additional weakening of the thermally induced LPG caused by gain saturation. The approximate expression for χ, calculated using Eq. (21), is seen to provide a reasonable approximation to the exact value. The approximation is seen to be better for a fiber with a reduced doped region of the core, which can be understood by considering the integral over the doped region in Eq. (19). For a smaller doped region, the approximation of a nearly constant FM profile over the doped area improves.

3. Solution of the coupled-mode equations

In order to solve the coupled-mode equations given by Eqns. (22) we make the approximation that the light in the FM is undepleted by TMI. Since the expansion in Eq. (13) is only valid for a weak excitation of the HOM, our model applies only to operation below or near the TMI threshold, and hence the approximation of an undepleted FM should be valid. In addition, we introduce a propagation equation for the pump light. We thus consider the following system of 3 coupled ODEs

$$\frac{\partial P_p}{\partial z} = \pm\frac{A_d}{A_{cl}}\tilde{g}_p(P_p,P_1)P_p, \tag{26a}$$

$$\frac{\partial P_1}{\partial z} = \Gamma_1\tilde{g}(P_p,P_1)P_1, \tag{26b}$$

$$\frac{\partial P_2}{\partial z} = \tilde{g}(P_p,P_1)\tilde{\chi}(z,\Delta\omega)P_1P_2 + \Gamma_2\tilde{g}(P_p,P_1)P_2, \tag{26c}$$

where A_{cl} is the area of the pump cladding and the positive/negative sign corresponds to co- and counter-pumped operation, respectively. The pump gain coefficient $\tilde{g}_p$ and the signal gain coefficient $\tilde{g}$ are found by solving the steady-state rate equations, and we assume here that ytterbium is used as the rare-earth dopant.

We can formally solve Eq. (26c) and, as in [11, 12], we assume that the instability is seeded by noise. We therefore integrate over all frequencies ω_2 to obtain the total output power in the HOM

$$P_2(L) = \int_{-\infty}^{\infty} S_2(0,\Delta\omega)\left(\frac{P_1(L)}{P_1(0)}\right)^{\Gamma_2/\Gamma_1}\exp\left(\chi_0(\Delta\omega)\int_0^L\frac{\tilde{g}^2}{g_0}P_1\mathrm{d}z\right), \tag{27}$$

where $S_2(0,\Delta\omega)$ is the input power spectral density of the light in the HOM and L is the fiber length. It was argued in [12] that a likely source for seeding the TMI is intensity noise in the input signal. In this case the input power spectral density is

$$S_2(0,\Delta\omega) = P_2(0)\delta(\Delta\omega) + \frac{1}{4}R_N(\Delta\omega)P_2(0), \tag{28}$$

which gives the following expression for the output HOM content $\xi = P_2(L)/[P_1(L)+P_2(L)]$

$$\xi(L) \approx \xi(0)\left(\frac{P_1(0)}{P_1(L)}\right)^{1-\Gamma_2/\Gamma_1}\left[1+\frac{R_N(\Omega)}{4}\sqrt{\frac{2\pi}{|\chi_0''(\Omega)|M}}\exp\left(\chi_0(\Omega)M\right)\right], \tag{29}$$

where Ω is the value of $\Delta\omega$ for which χ_0 has its maximum value, χ_0'' is the second derivative of χ_0 with respect to $\Delta\omega$ and M is given by the integral

$$M = \int_0^L\frac{\tilde{g}^2}{g_0}P_1\mathrm{d}z. \tag{30}$$

This integral is evaluated by first solving Eqns. (26a) and (26b) numerically using a standard numerical ODE solver followed by numerical quadrature. Likewise, the integral in Eq. (25)

#205315 - $15.00 USD Received 24 Jan 2014; revised 4 Apr 2014; accepted 25 Apr 2014; published 2 May 2014

required for calculating χ_0 is evaluated for a range of frequencies using standard numerical quadrature techniques.

We calculated the HOM content $\xi(L)$ as a function of output signal power for the fiber given in Table 1. The result is shown in Fig. 2 for both co- and counter-pumped operation, and is also compared to the result obtained when the effect of the gain oscillations are neglected as in [11,12]. The input signal power was taken to be 10 W and the input HOM content $\xi(0) = 0.01$, which should correspond to nearly optimal coupling of the signal into the fiber core. The relative intensity noise was assumed to be -100 dBc/Hz, which we believe is representative of realistic experimental conditions. Defining the TMI threshold power P_{th} as the output signal power at which $\xi(L) = 0.1$, we find $P_{th} = 723$ W for counter-pumped operation and $P_{th} = 672$ W for co-pumped operation. Compared to the corresponding value of $P_{th} = 260$ W obtained when gain oscillations are neglected, it is clear that this effect is very important in this case. Interestingly, there is little difference in TMI threshold between the co- and counter-pumped cases. When gain saturation is low and the effect of the associated gain oscillations can be ignored, this is expected, as shown in [11]. Apparently, including the effects of gain saturation in the model approximately preserves the symmetry between co- and counter-pumping.

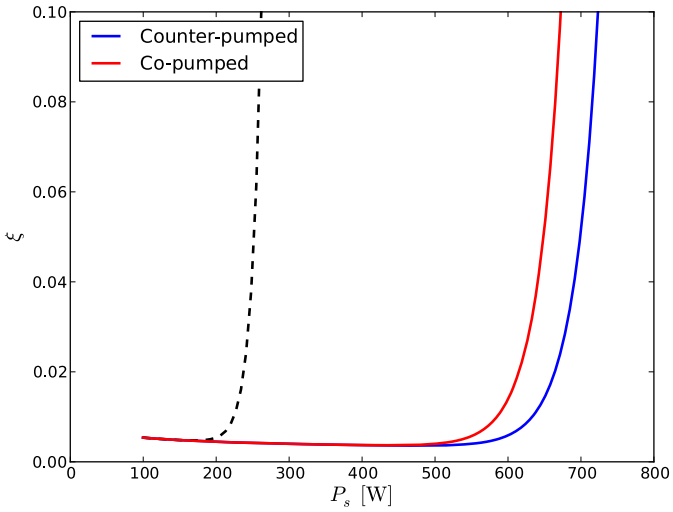

Fig. 2. HOM content ξ as a function of signal output power P_s for Fiber A for counter-pumped (blue curve) and co-pumped (red curve) operation. The dashed curve shows the result when the gain oscillations are neglected as in [11, 12].

We have also performed the same calculation for Fiber B. The result is shown in Fig. 3. The TMI thresholds for co- and counter-pumped operation are 1047 W and 1286 W, respectively, which is substantially higher than for Fiber A. This is due to the combination of the reduced overlap between the modes with the doped region and the longer fiber length. From the dashed curve in Fig. 3 we see that the TMI threshold, calculated under the assumption of negligible gain oscillations, is 331 W for Fiber B. This increase of 27% compared to Fiber A is due to the reduced mode overlap with the doped region. However, the increase in TMI threshold when taking gain oscillations into account is much larger, 78% for counter-pumped and 56% for co-pumped. This increase in TMI threshold thus cannot solely be explained by the reduced mode overlap, but is also caused by the higher gain saturation. We have verified this conclusion by simulating a shorter version of Fiber B, which has the same length as Fiber A. In this case, the

#205315 - $15.00 USD Received 24 Jan 2014; revised 4 Apr 2014; accepted 25 Apr 2014; published 2 May 2014

TMI threshold for co-pumped operation drops to 767 W compared to 1047 W for the original Fiber B. This is due to the fact that the gain is much less saturated in this case, which in turn implies that the gain oscillations are weaker and the thermally induced LPG is stronger. However, this shorter version of Fiber B has a very poor efficiency due to the lower pump absorption, and is thus not considered a realistic case.

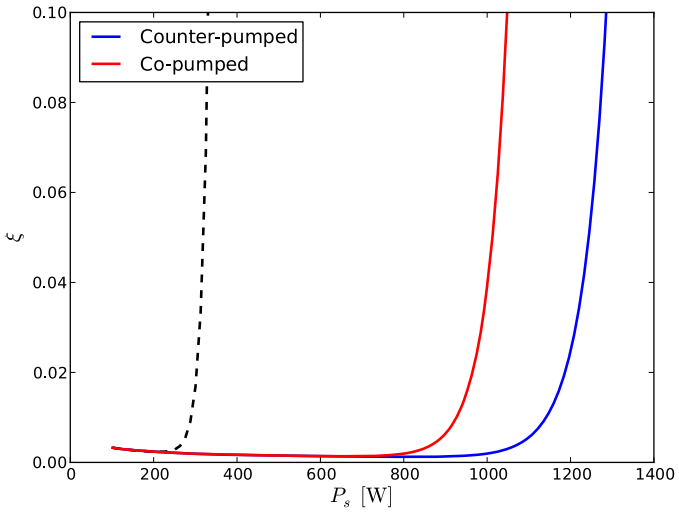

Fig. 3. HOM content ξ as a function of signal output power P_s for Fiber B for counter-pumped (blue curve) and co-pumped (red curve) operation. The dashed curve shows the result when the gain oscillations are neglected as in [11, 12].

4. Comparison to BPM calculations by Smith and Smith

In a recent paper [13], Smith and Smith investigated the effect of gain saturation on TMI numerically using a BPM code. In this section we compare our calculation of the nonlinear gain coefficient χ with a calculation of the same quantity obtained by the BPM presented in Fig. 5 in [13]. The fiber parameters for the two SIFs used for the comparison are given in Table 2. The first fiber, here called Fiber C, is a short fiber with a small pump cladding, which provides high pump intensity and hence lower gain saturation, while the second fiber, called Fiber D, is a longer fiber with a much larger pump cladding, which therefore operates with much higher gain saturation. We have calculated the nonlinear gain coefficient χ using the approximate expression given in Eq. (21) as a function of z for a fixed frequency offset $\Delta\nu = 1.1$ kHz and the specific pump powers given in [13]. The result for Fiber C is shown in Fig. 4, while the result for Fiber D is shown in Fig. 5. Compared to Fig. 5 in [13] we find a reasonably good agreement with our results, but with some interesting differences. For Fiber C, we find an initially lower value of χ for the counter-pumped case, which rises to a slightly lower value than in [13]. For the co-pumped case, χ falls off more quickly with z compared to [13] and also reaches a lower value. The same is true for the co-pumped case for Fiber D, while the counter-pumped case shows an initial value of χ slightly higher than in [13], which then falls off with z to a slightly lower value. Interestingly, the counter-pumped case in the lower plot of Fig. 5 in [13] shows a slightly *increasing* nonlinear gain χ with z, which according to our analysis would seem to indicate a *decreasing* gain saturation with z. However from Fig. 2 in [13], it appears that the

#205315 - $15.00 USD Received 24 Jan 2014; revised 4 Apr 2014; accepted 25 Apr 2014; published 2 May 2014

Table 2. Fiber parameters for Fiber C and D used for comparison with [13].

Core radius	R_{core}	25 μm
Cladding radius	R_{clad}	50 μm / 200 μm
Doped radius	R_{doped}	25 μm
Outer radius	R_{outer}	500 μm
Core index	n_{core}	1.451
V parameter	V	8.2
Dopant concentration	ρ_{Yb}	3×10^7 μm^{-3}
Fiber length	L	0.8 m / 4 m
Signal wavelength	λ_s	1032 nm
Pump wavelength	λ_p	976 nm

gain saturation is in fact *increasing* with z. A possible explanation of this apparent discrepancy could be thermal lensing, since the larger heat load toward the output end of the fiber will cause the overlap between the HOM and FM to increase, which will increase the nonlinear gain.

To test the accuracy of the approximate calculation of χ for Fiber C and D, we again compare the exact and approximate expressions for a fixed frequency offset $\Delta\nu = 1.1$ kHz and for a range of values of P_1/P_{sat}. The result is shown in Fig. 6 and shows good agreement between the exact and approximate calculations even when gain saturation is substantial. The discrepancy between the calculation in [13] and our model is thus unlikely to be due to this approximation, but is rather due to other approximations, such as the fact that we do not include thermal lensing, and the fact that we treat the gain oscillations to first order only.

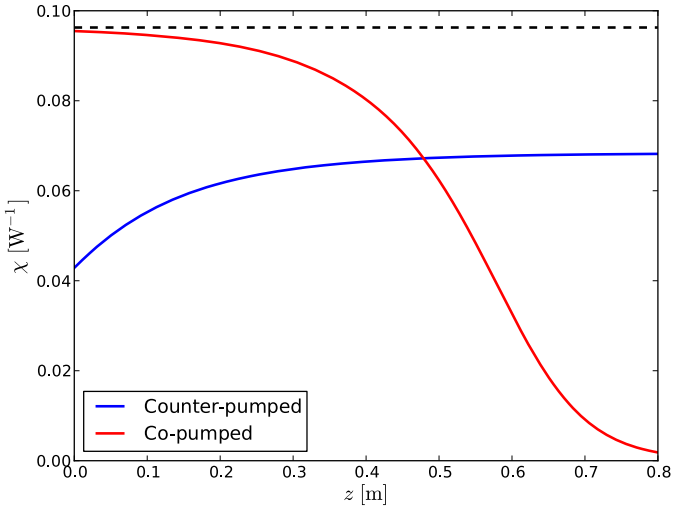

Fig. 4. Nonlinear gain coefficient χ as a function of z for Fiber C. The blue curve is for counter-pumped operation with a pump power of 493 W, and the red curve is for co-pumped operation with a pump power of 525 W. The dashed curve shows the value of χ_0.

#205315 - $15.00 USD Received 24 Jan 2014; revised 4 Apr 2014; accepted 25 Apr 2014; published 2 May 2014

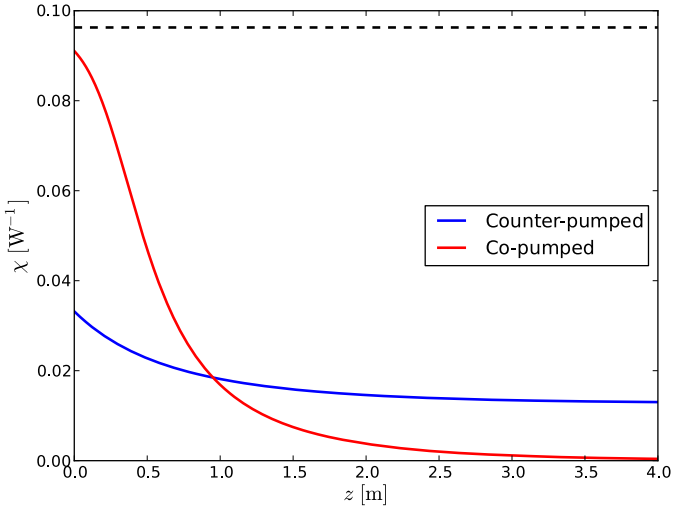

Fig. 5. Nonlinear gain coefficient χ as a function of z for Fiber D. The blue curve is for counter-pumped operation with a pump power of 1350 W, and the red curve is for co-pumped operation with a pump power of 1200 W. The dashed curve shows the value of χ_0.

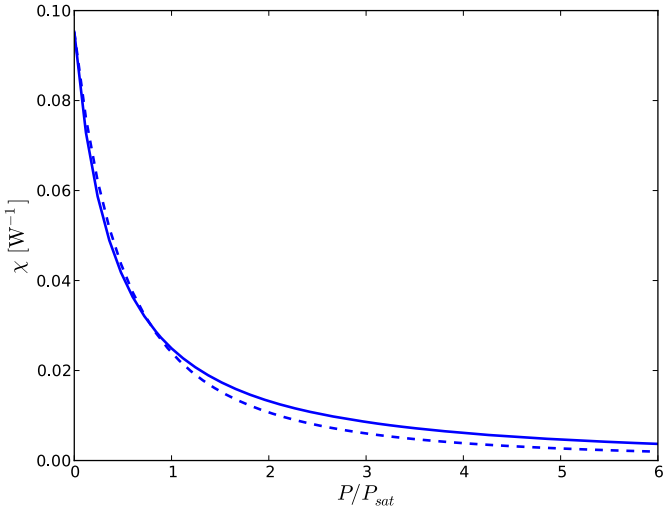

Fig. 6. Nonlinear gain coefficient χ at a fixed frequency offset $\Delta\nu = 1$ kHz as a function of P_1/P_{sat} for Fiber C and D. The solid curve is calculated using the exact expression, and the dashed curved is calculated using the approximate expression.

5. Conclusion

In summary we have shown how the effects of gain saturation can be included approximately in a coupled-mode model of TMI. The resulting model is numerically very efficient and easy

#205315 - $15.00 USD Received 24 Jan 2014; revised 4 Apr 2014; accepted 25 Apr 2014; published 2 May 2014

to implement, and can be used to obtain quantitative estimates of the TMI threshold for a given fiber amplifier under conditions where gain saturation is substantial. Applying our model to particular SIF designs (Fiber A & B), we found that the estimate for the TMI threshold increased by approximately a factor of 3 compared to a model which does not include the effect of gain saturation. Only in the case of a short, rod-type fiber (Fiber C) did we find a nonlinear gain comparable to the prediction of the model when neglecting gain saturation effects. We also found that the benefit of reducing the doped area of the core is significantly greater than predicted by the simpler model, due to the increased gain saturation. Including gain saturation in the model breaks the symmetry between co- and counter-pumping, with the latter having the higher TMI threshold.

Comparing our model to BPM simulations presented in [13], we found reasonably good agreement between the nonlinear gain coefficient calculated with our model and the BPM results, although our model results in slightly lower values for the nonlinear gain coefficient. This is likely due to the various approximations employed by our model, most importantly the neglect of thermal lensing and the fact that gain saturation is only included to lowest order of approximation. We thus expect our model to be able to provide good quantitative estimates of the TMI thresholds of fiber amplifier designs under conditions where gain saturation is significant.

#205315 - $15.00 USD Received 24 Jan 2014; revised 4 Apr 2014; accepted 25 Apr 2014; published 2 May 2014